Biochemical and Biophysical Research Communications 464 (2015) 336–341

Contents lists available at ScienceDirect

Biochemical and Biophysical Research Communications

journal homepage: www.elsevier.com/locate/ybbrc

Changes in secondary structure of α-synuclein during oligomerization induced by reactive aldehydes

Yixiao Cai [a], Christofer Lendel [b], Lars Österlund [a], Alex Kasrayan [c], Lars Lannfelt [d], Martin Ingelsson [d], Fredrik Nikolajeff [a], Mikael Karlsson [a], Joakim Bergström [d, *]

[a] Department of Engineering Sciences, Ångström Laboratory, Uppsala University, Sweden
[b] Department of Chemistry, KTH Royal Institute of Technology, Stockholm, Sweden
[c] BioArctic Neuroscience, Stockholm, Sweden
[d] Department of Public Health and Caring Sciences, Rudbeck Laboratory, Uppsala University, Sweden

ARTICLE INFO

Article history:
Received 19 June 2015
Accepted 24 June 2015
Available online 27 June 2015

Keywords:
Alpha-synuclein
Oligomers
Aggregation
Amyloid
Oxidative stress
4-Hydroxy-2-nonenal
4-Oxo-2-nonenal
Parkinson's disease
Dementia with Lewy bodies

ABSTRACT

The oxidative stress-related reactive aldehydes 4-hydroxy-2-nonenal (HNE) and 4-oxo-2-nonenal (ONE) have been shown to promote formation of α-synuclein oligomers *in vitro*. However, the changes in secondary structure of α-synuclein and the kinetics of the oligomerization process are not known and were the focus of this study. Size exclusion chromatography showed that after 1 h of incubation, HNE induced the formation of an oligomeric α-synuclein peak with a molecular weight of about ~2000 kDa, which coincided with a decreasing ~50 kDa monomeric peak. With prolonged incubation (up to 24 h) the oligomeric peak became the dominating molecular species. In contrast, in the presence of ONE, a ~2000 oligomeric peak was exclusively observed after 15 min of incubation and this peak remained constant with prolonged incubation. Western blot analysis of HNE-induced α-synuclein oligomers showed the presence of monomers (15 kDa), SDS-resistant low molecular (30–160 kDa) and high molecular weight oligomers (≥260 kDa), indicating that the oligomers consisted of both covalent and non-covalent protein. In contrast, ONE-induced α-synuclein oligomers only migrated as covalent cross-linked high molecular-weight material (≥300 kDa). Both circular dichroism (CD) and Attenuated total reflectance Fourier transform infrared (ATR-FTIR) spectroscopy showed that the formation of HNE- and ONE-induced oligomers coincided with a spectral change from random coil to β-sheet. However, ONE-induced α-synuclein oligomers exhibited a slightly higher degree of β-sheet. Taken together, our results indicate that both HNE and ONE induce a change from random coil to β-sheet structure that coincides with the formation of α-synuclein oligomers; albeit through different kinetic pathways depending on the degree of cross-linking.

1. Introduction

Aggregated α-synuclein is the main component of Lewy bodies and Lewy neurites; cytoplasmic inclusions found in affected neurons in Parkinson's disease (PD) and dementia with Lewy bodies (DLB) [1,2]. The α-synuclein protein consists of 140 amino acid residues and can be divided into three different regions: a lipid binding N-terminal (1–60), a hydrophobic core region (61–95) and a negatively charged C-terminus (96–140). Although the exact physiological function of α-synuclein is not completely clear, increasing evidence suggest that α-synuclein interacts with membranes regulating the synaptic vesicle recycling pool and the release of neurotransmitters by promoting SNARE complex assembly [3,4].

Genetic evidence implicate α-synuclein as the key player in the disease pathogenesis of PD and DLB. Point mutations or multiplications of the *wild type* gene are linked to early onset forms of either PD (*A30P*, *H50Q*, *G51D*, *A53E*, *A53T* and *wild type* duplications) or DLB (*E46K* and *wild type* triplications) [5]. The initiating step in the aggregation process of α-synuclein is believed to be the formation of a partially folded intermediate species that is capable of self-assembling into oligomeric and fibrillary structures [6,7]. A common denominator of the α-synuclein mutations are that they increase the oligomerization rate of the protein *in vitro* [8].

* Corresponding author.
E-mail address: joakim.bergstrom@pubcare.uu.se (J. Bergström).

http://dx.doi.org/10.1016/j.bbrc.2015.06.154
0006-291X/

Furthermore, increasing evidence imply that oligomeric forms of α-synuclein are the most neurotoxic molecular species *in vivo* [9,10].

Oxidative stress has been linked to both idiopathic and familial forms of Parkinson's disease [11,12]. For example, decreased levels of glutathione, the major reducing agent in the cell, can be observed in the substantia nigra of PD brains [13]. Moreover, the levels of oxidized lipids have been shown to be elevated in cortical neurons in DLB [14]. Proteins modified by the lipid peroxidation end product 4-hydroxy-2-nonenal (HNE) can be found to a higher degree in Lewy bodies in the substantia nigra of PD brains and in neocortical and brainstem Lewy bodies in DLB [15–17]. Alpha-synuclein may itself be a contributor to oxidative stress, as over expression of the protein in transgenic mice and various cell models leads to an impaired mitochondrial function [18,19].

It has been shown that HNE, and the chemically related reactive aldehyde 4-oxo-2-nonenal (ONE) [20], can induce the formation of α-synuclein oligomers *in vitro* [21–25]. However, the kinetics of the oligomerization process have not been fully elucidated. Furthermore, a discrepancy regarding the secondary structure of the α-synuclein oligomers formed in the presence of HNE has been reported. They have shown to either have an ordered secondary structure with a high β-sheet content [21–23], or a disordered secondary structure with little β-sheet structure [24,25]. The aim of the current study was to characterize the kinetics and the secondary structural changes of HNE- and ONE-induced α-synuclein oligomerization.

2. Material and methods

2.1. Chemicals

HNE (10 mg/ml) was supplied in 99% ethanol and ONE (5 mg/ml) in 99% methyl acetate (Cayman Chemical, Ann Arbor, MI).

2.2. Modification of α-synuclein with HNE/ONE and generation of fibrillar α-synuclein

Recombinant α-synuclein was expressed as described earlier [22]. Monomeric α-synuclein (140 μM) in 50 mM phosphate buffer pH 7.4 was incubated with either HNE or ONE at a 1:30 (α-synuclein:aldehyde) excess and the samples were quiescently incubated at 37 °C for 15 min, 1 h, 3 h, 6 h and 24 h. Alpha-synuclein fibrils were generated as previously described [22].

2.3. Size exclusion chromatography-high performance liquid chromatography (SEC-HPLC)

Alpha-synuclein samples incubated with HNE or ONE were diluted to 20 μM using 50 mM Tris/0.15 M NaCl, pH 7.4 and 10 μL was injected onto a Superose 6 PC 3.2/30 column (GE Healthcare, Uppsala, Sweden) using a Merck Hitachi D-7000 HPLC LaChrom system with a diode array detector (VWR, Stockholm, Sweden). As mobile phase, a 50 mM Tris/0.15 M NaCl, pH 7.4 buffer was used with a flow rate of 50 μl/min and the UV absorbance was monitored at 214 nm. A low and high molecular weight gel filtration calibration kit (GE Healthcare, Uppsala, Sweden) was used to estimate the molecular weight of the various α-synuclein species. Peak areas were integrated using Merck Hitachi model D-7000 chromatography data station software. The experiment was repeated three times and typical data is shown.

2.4. Western blot and dot blot analysis

One hundred ng of unmodified, HNE- or ONE-treated or fibrillar α-synuclein was dissolved in SDS- and dithiothreitol-containing sample buffer, followed by boiling at 95 °C for 5 min. Next, proteins were separated on a Bolt 4–12% Bis-Tris Plus gel (Life Technologies, Carlsbad, CA) and transferred to a 0.2 μM Amersham Protran premium nitrocellulose membrane (GE Healthcare). For dot blot analysis, 100 ng of the samples were dropped on to a 0.2 μM Amersham Protran premium nitrocellulose membrane (GE Healthcare). The western blot and the dot blot were visualized in an Odyssey® Sa infrared imaging system (Li-Cor, Lincoln, NE) using an α-synuclein polyclonal antibody (0.2 μg/ml, sc-7011-R; Santa Cruz Biotechnology, Santa Cruz, CA) followed by a secondary antibody (donkey anti-rabbit, 0.2 μg/ml, IRDye 800CW; Li-Cor). The experiments were repeated three times and typical data is shown.

2.5. Circular dichroism (CD)

HNE- or ONE-treated α-synuclein were diluted to a final concentration of 15 μM in 50 mM phosphate, pH 7.4. The far-UV CD spectra (between 250 and 190 nm) were recorded on a Jasco J-810 spectrometer (Jasco, Easton, MD) with a step size of 0.1 nm using a cuvette with a 1-mm path length. Each scan was repeated three times to reduce noise and the background value of the phosphate buffer was subtracted for all measurements. All data are presented as a mean value per nanometer recorded. All the spectra were recorded at 25 °C.

2.6. Attenuated total reflection Fourier transform infrared (ATR-FTIR) spectroscopy

The attenuated total reflection Fourier transform infrared (ATR-FTIR) spectra were measured on a vacuum-pumped FTIR spectrometer (Bruker IFS 66v/S, Ettlingen, Germany) equipped with a commercial 9 reflections ATR diamond crystal cell (Smiths Detection, Edgewood, MD). The sample compartment was evacuated to 1 mbar prior to acquisition in order to remove water vapor contribution from the spectra. Each spectrum was averaged over 1024 scans. The spectra were collected at room temperature with a resolution of 2 cm^{-1}. The protein samples analyzed by ATR-FTIR included monomeric, HNE- or ONE-treated and fibrillar α-synuclein. In each experiment 10 μl of the protein sample was pipetted on top of the ATR crystal. The spectra were recorded at least two times for each sample. The OPUS IR-software (Bruker Optics GmbH) was used to analyze the spectra. The water vapor component was subtracted from each of the sample spectra and the amide I region between 1700 and 1600 cm^{-1} were extracted after baseline correction. The ratio of the 1625 cm^{-1} and 1650 cm^{-1} bands as a function of incubation time were calculated for HNE- and ONE-treated α-synuclein with the assumption that the ATR-FTIR spectrum of fibrils was associated with 100% β-sheet and the monomeric protein with 100% α-helix/random coil structure.

3. Results

3.1. SEC-HPLC analysis of HNE- or ONE-treated α-synuclein

Size exclusion chromatography showed that after 15 min of incubation with HNE, α-synuclein eluted as a monomeric peak at 50 kDa (Fig. 1A), similar to the unmodified protein (data not shown). The apparent molecular weight of the monomer was higher than expected, as the calculated molecular weight of α-synuclein is 14460 Da. However, this finding can be explained by the fact that monomeric α-synuclein adopts an extended conformation in solution [26]. With prolonged incubation (≥1 h), the 50 kDa monomeric peak decreased and an oligomeric peak with a molecular weight of about ~2000 kDa could be observed (amount of oligomers formed at the various time points: 1 h–9%, 3 h–58%,

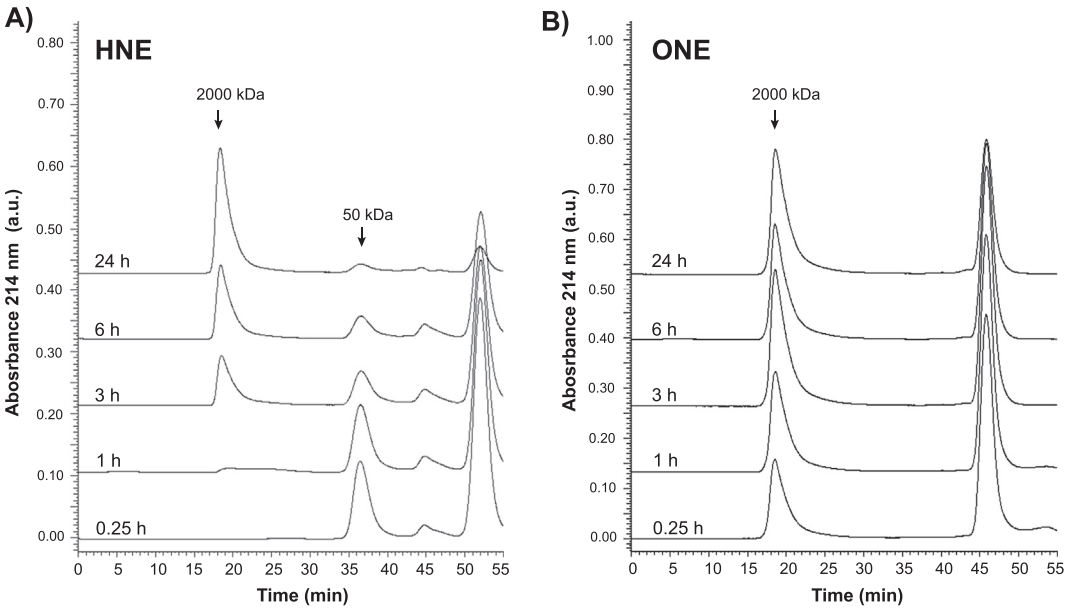

Fig. 1. Size exclusion analysis of HNE- and ONE-treated α-synuclein at 15 min, 1 h, 3 h, 6 h and 24 h. After 15 min, only a 50 kDa monomeric peak, similar to for unmodified protein (data not shown), was observed in the HNE-treated α-synuclein sample (A). With prolonged incubation, the monomeric peak decreased and a ~2000 kDa oligomeric peak became the dominating molecular species (A). At all the time points, ONE-treated α-synuclein eluted as an oligomeric peak with a molecular weight of about ~2000 kDa (B). Peaks representing unbound HNE (45/52 min) and ONE (45 min) were observed at all the time points.

6 h—81%, 24 h—97%). In contrast, after 15 min of incubation with ONE, α-synuclein eluted exclusively as an oligomeric peak with a molecular weight of ~2000 kDa (Fig. 1B). This peak remained constant throughout the experiment and thus no monomeric protein could be detected at any time point with ONE-treated α-synuclein samples.

3.2. *Western blot and dot blot analysis of native, HNE- or ONE-treated and fibrillar α-synuclein*

In western blot analysis, unmodified α-synuclein migrated as a monomeric band around 15 kDa (Fig. 2A). Western blot analysis of HNE-treated α-synuclein showed that besides monomeric protein at 15 kDa, low molecular weight oligomers (up to octamers around 180 kDa) could be observed after 15 min of incubation (Fig. 2A). With prolonged incubation, the oligomeric bands increased in intensity and after ≥3 h a high molecular smear (≥260 kDa) could also be observed. After 24 h, less immunoreactive material was observed overall. However, a band at the edge at the well (≥300 kDa) was also detected, indicative of the formation of high molecular weight α-synuclein species not entering the separation gel. In ONE-treated α-synuclein samples, a high molecular weight material was observed at the edge of the well (Fig. 2A). With increasing incubation (≥6 h) this band increased in intensity, whereas a fainter smear below disappeared. No monomeric α-synuclein was observed at any time point in the ONE-treated

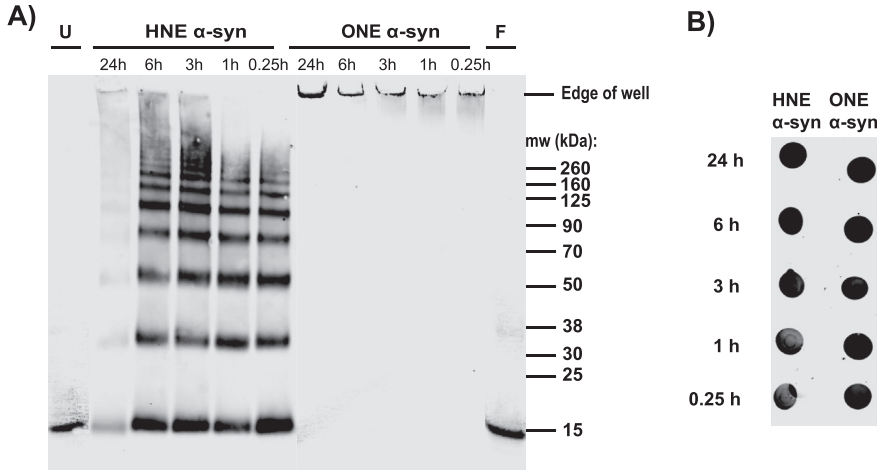

Fig. 2. Western blot and dot blot analysis of monomeric, HNE- or ONE-treated and fibrillar α-synuclein. Initially, HNE-treated α-synuclein migrated as a monomer and low molecular-weight oligomers (up to octamers) (A). With prolonged incubation, the low molecular-weight (up to 180 kDa) oligomers increased in intensity and a high molecular-weight smear also became visible (≥260 kDa). ONE-treated α-synuclein migrated mainly as a high molecular-weight material (≥300 kDa) at the edge of the well. With prolonged incubation, this band increased in intensity whereas a fainter smear below disappeared. Unmodified (U) and fibrillar (F) α-synuclein migrated predominantly as 15 kDa monomeric band. Dot blot analysis verified that similar amounts of HNE- or ONE-treated α-synuclein were analyzed by western blot (B).

samples. In α-synuclein fibril samples, the dominating species was a monomeric band at 15 kDa, but a faint dimeric band could also be detected (Fig. 2A). A dot blot verified that similar amounts of HNE- or ONE-treated α-synuclein samples were analyzed in the western blot (Fig. 2B).

3.3. CD analysis of HNE- or ONE-treated α-synuclein

After 15 min of incubation with HNE, α-synuclein exhibited a CD spectrum with a distinct minimum in the vicinity of 198 nm (Fig. 3A). This is typical of a random coil polypeptide chain and similar to what we previously have shown for unmodified monomeric α-synuclein protein [22]. However, after 3 h of incubation, the minimum at 198 nm disappeared and a new minimum with a broad appearance around 216 nm, indicative of β-sheet structure, could be observed. With prolonged incubation up to 24 h, the negative ellipticity around 216 nm increased in intensity. In contrast, α-synuclein samples incubated with ONE showed a more well-defined minimum around 217 nm already after 15 min of incubation and it remained constant at all subsequent time points (Fig. 3B).

3.4. ATR-FTIR analysis of natively structured, HNE- or ONE-treated and fibrillar α-synuclein

The ATR-FTIR spectrum of unmodified α-synuclein showed a broad band centered at 1650 cm^{-1}, indicating predominantly random coil and/or α-helix secondary structure (Fig. 4A). In addition, a shoulder around 1625 cm^{-1}, characteristic of β-sheet structure, was also evident. After 15 min, HNE-treated α-synuclein showed two main peaks at 1625 cm^{-1} and 1650 cm^{-1} with about equal amplitude (Fig. 4B). With prolonged incubation, the peak at 1625 cm^{-1} increased in intensity, indicating the formation of β-sheet structure, whereas the peak at 1650 cm^{-1} decreased in intensity (β-sheet content at the different time points: 15 min–8%, 1 h–10%, 3 h–12%, 6 h–15%, 24 h–13%). In contrast, the ATR-FTIR spectra of ONE-treated α-synuclein showed a main peak at 1625 cm^{-1} and a smaller peak around 1650 cm^{-1} at all the time points (β-sheet content at the different time points: 15 min–22%, 1 h–21%, 3 h–23%, 6 h–23%, 24 h–24%) (Fig. 4C). In addition, a shoulder peak at 1695 cm^{-1} could be observed for both HNE- and ONE-treated α-synuclein samples throughout the experiment (Fig. 4B, C). For fibrillar α-synuclein, a single band at 1625 cm^{-1} was seen (Fig. 4D).

4. Discussion

Both native and aggregated forms of α-synuclein are found closely associated with the cell membrane [4,27]. Interestingly, the highest levels of reactive aldehydes such as HNE and ONE can be found in the vicinity of neuronal cell membranes [20,28]. HNE and ONE have a very similar chemical structure, they only differ at the C4 position where HNE has a hydroxyl group and ONE a carbonyl group. However, this chemical property renders ONE more prone to cross-link proteins [20]. Interestingly, the α-synuclein oligomers induced by HNE and ONE differ in structure, compactness and morphology [21,22]. Furthermore, conflicting results have been reported regarding the secondary structure of HNE-induced α-synuclein oligomers; as they have been suggested to either have an extended β-sheet structure or exhibit an unfolded structure [22–24]. In addition, the rate of oligomerization of α-synuclein induced by HNE and ONE has not been fully elucidated. Hence, the aim of the present study was to study the kinetics and structural changes of α-synuclein during oligomer formation induced by HNE and ONE.

By using size exclusion chromatography, the oligomerization process can be studied under native conditions. For HNE, large sized (~2000 kDa) α-synuclein oligomers could first be observed after 1 h of incubation with HNE. This oligomeric peak increased in size with prolonged incubation and after 24 h only a minimal monomeric peak was observed. In contrast, the kinetics of ONE-induced oligomerization differed drastically. After only 15 min of incubation with ONE, all monomeric α-synuclein had been converted into a large (~2000 kDa) oligomeric peak that did not change in appearance with prolonged incubation. With the denaturing western blot method, the SDS stability (i.e. the degree of cross-linking) of the formed α-synuclein oligomers can be determined. For HNE-treated α-synuclein, apart from a distinct monomeric band, low molecular weight α-synuclein oligomers (up to octamers) could be observed at an early stage (after 15 min). However, the fact that oligomers at this time point only could be detected with the more sensitive western blot method indicates that they had been formed in minute amounts. With prolonged incubation, the amount of low molecular weight oligomers increased, and in addition, a high-molecular weight smear could also be observed; thus indicating an overall increase in cross-linking. However, as monomeric protein was detected at all the time points, also non-covalently bound α-synuclein was part of the oligomeric structure. In contrast, for ONE-treated α-synuclein only a high molecular weight material not entering the gel could be seen throughout the experiment. Together with the finding that no monomeric protein was observed at any time point, our data clearly show that ONE

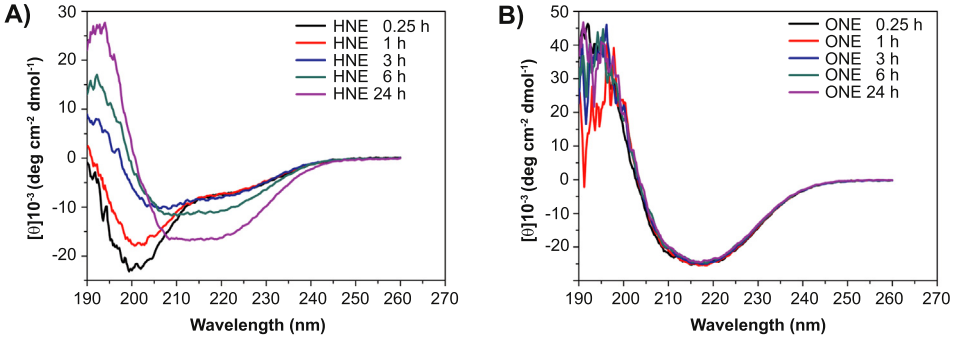

Fig. 3. Far-UV CD analysis of HNE- or ONE-treated α-synuclein at the different time points. For HNE-treated α-synuclein, a minimum in the ellipticity around ~198 nm was found initially (up to 1 h), but with prolonged incubation a conversion to a broad minimum in the ellipticity at ~216 nm could be observed (A). All the ONE-treated α-synuclein samples exhibited a distinct minimum in the ellipticity at ~217 nm (B).

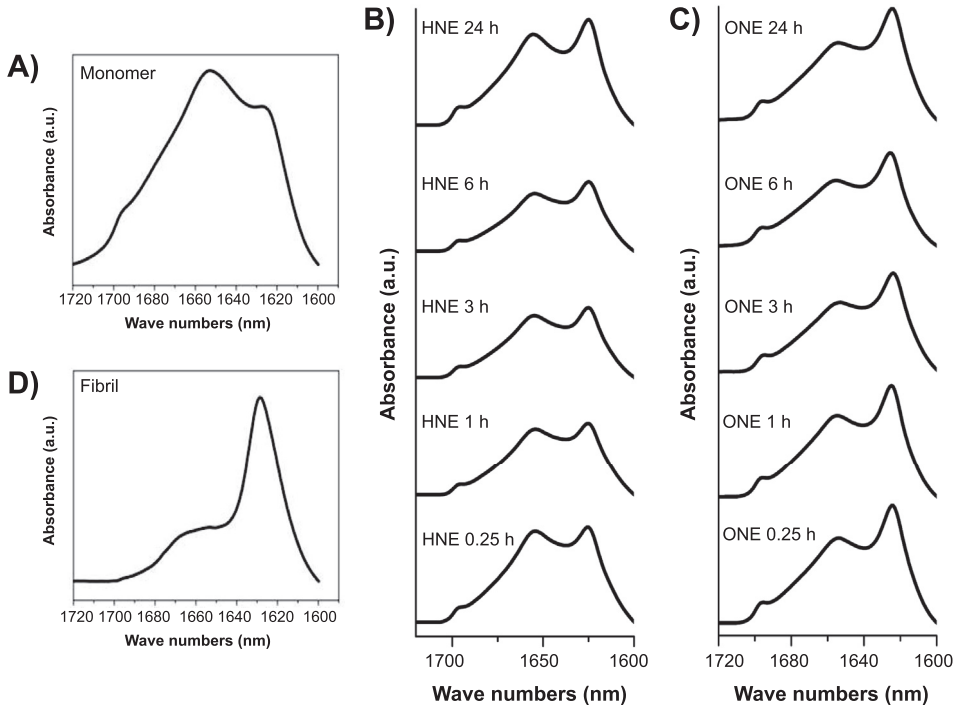

Fig. 4. ATR-FTIR analysis of monomeric, HNE- or ONE-treated and fibrillar α-synuclein. Unmodified monomeric α-synuclein had a peak centered at 1650 cm^{-1} (A). Initially, HNE-treated α-synuclein showed two main peaks at 1625 cm^{-1} and 1650 cm^{-1} (B). With prolonged incubation, the peak at 1625 cm^{-1} increased in intensity (B). The spectra for ONE-treated α-synuclein showed a main peak at 1625 cm^{-1} and a smaller peak at 1650 cm^{-1} at all the time points (C). Fibrillar α-synuclein exhibited one peak around 1625 cm^{-1} (D).

induced α-synuclein oligomers were covalently cross-linked to a much higher degree. In contrast, fibrillar α-synuclein formed from the unmodified protein showed little evidence of cross-linking, as mainly a monomeric band could be observed under denaturing conditions.

According to the CD and FTIR data, a change from α-helix/random coil to a β-sheet structure coincided with the formation of HNE- and ONE-induced oligomers. Interestingly, despite forming much faster, due to a higher degree of cross-linking, ONE-induced α-synuclein oligomers displayed a slightly higher β-sheet content compared to HNE-induced oligomers. However, fibrillar α-synuclein exhibited a much more pronounced β-sheet structure compared to both HNE- and ONE-induced α-synuclein oligomers according to ATR-FTIR data. Furthermore, both HNE- and ONE-induced oligomers, but not α-synuclein fibrils, exhibited a weak band at 1695 cm^{-1}, which is indicative of an anti-parallel β-sheet structure. Taken together, our ATR-FTIR data show that the α-synuclein oligomers formed in the presence of either HNE or ONE differ in secondary structure from fibrils formed by the unmodified protein. This observation agrees well with our earlier findings that neither HNE- nor ONE-induced α-synuclein oligomers were capable of forming fibrils, even with prolonged incubation [22]. Notably, conflicting results have been reported regarding the secondary structure of HNE-induced α-synuclein oligomers [22–24]. Our data clearly indicate that HNE-induced α-synuclein oligomers have a β-sheet structure and that the change in secondary structure coincides with their formation. The discrepancy observed between studies is not easy to explain, but could be due to differences in α-synuclein purity, chemicals used etc. Furthermore, here we show for the first time that ONE-induced α-synuclein oligomers exhibit a distinct β-sheet structure already upon their formation.

Several other chemical compounds, such as polyphenol (−)-epigallocatechin gallate and dopamine, have been shown to induce the formation of non-fibrillating (i.e. “off-pathway”) α-synuclein oligomers [29,30]. However, in contrast to the aldehyde-induced α-synuclein in the present study, they usually lack an ordered secondary structure [29,30]. One exception is baicalein, which also can induce α-synuclein oligomers with significant β-sheet content [31]. However, whereas baicalein have shown to have a little effect on membrane integrity [31], both HNE- and ONE-induced α-synuclein oligomers have been shown to be neurotoxic *in vitro* [22,23,25,32]. Thus it is possible that oligomers formed in the presence of such reactive aldehydes may exhibit particularly noxious properties compared to other off-pathway α-synuclein oligomers. Taken together, the current study shows that although both aldehydes induce α-synuclein oligomers that exhibit β-sheet structure, the oligomers promoted by ONE form much faster and display a slightly higher β-sheet content.

Acknowledgments

The work was supported financially by grants from China Scholarship Council (CSC) for the PhD fellowship, Uppsala Berzelii Technology Center for Neurodiagnostics, Swedish Parkinson Foundation, Swedish Alzheimer Foundation, Swedish Brain Foundation, Stohne's Foundation, Åhlén Foundation, Marianne and Marcus Wallenberg Foundation and Lennart and Christina Kalén.

Transparency document

Transparency document related to this article can be found online at http://dx.doi.org/10.1016/j.bbrc.2015.06.154.

References

[1] M.G. Spillantini, M.L. Schmidt, V.M. Lee, J.Q. Trojanowski, R. Jakes, M. Goedert, Alpha-synuclein in Lewy bodies, Nature 388 (1997) 839–840.

[2] A. Takeda, M. Mallory, M. Sundsmo, W. Honer, L. Hansen, E. Masliah, Abnormal accumulation of NACP/alpha-synuclein in neurodegenerative disorders, Am. J. Pathol. 152 (1998) 367–372.
[3] V.M. Nemani, W. Lu, V. Berge, K. Nakamura, B. Onoa, M.K. Lee, F.A. Chaudhry, R.A. Nicoll, R.H. Edwards, Increased expression of alpha-synuclein reduces neurotransmitter release by inhibiting synaptic vesicle reclustering after endocytosis, Neuron 65 (2010) 66–79.
[4] J. Burre, M. Sharma, T. Tsetsenis, V. Buchman, M.R. Etherton, T.C. Sudhof, Alpha-synuclein promotes SNARE-complex assembly in vivo and in vitro, Science 329 (2010) 1663–1667.
[5] W. Xu, L. Tan, J.T. Yu, The link between the SNCA gene and parkinsonism, Neurobiol. Aging 36 (2015) 1505–1518.
[6] V.N. Uversky, J. Li, A.L. Fink, Evidence for a partially folded intermediate in alpha-synuclein fibril formation, J. Biol. Chem. 276 (2001) 10737–10744.
[7] V.N. Uversky, H.J. Lee, J. Li, A.L. Fink, S.J. Lee, Stabilization of partially folded conformation during alpha-synuclein oligomerization in both purified and cytosolic preparations, J. Biol. Chem. 276 (2001) 43495–43498.
[8] D.F. Lazaro, E.F. Rodrigues, R. Langohr, H. Shahpasandzadeh, T. Ribeiro, P. Guerreiro, E. Gerhardt, K. Krohnert, J. Klucken, M.D. Pereira, B. Popova, N. Kruse, B. Mollenhauer, S.O. Rizzoli, G.H. Braus, K.M. Danzer, T.F. Outeiro, Systematic comparison of the effects of alpha-synuclein mutations on its oligomerization and aggregation, PLoS Genet. 10 (2014) e1004741.
[9] B. Winner, R. Jappelli, S.K. Maji, P.A. Desplats, L. Boyer, S. Aigner, C. Hetzer, T. Loher, M. Vilar, S. Campioni, C. Tzitzilonis, A. Soragni, S. Jessberger, H. Mira, A. Consiglio, E. Pham, E. Masliah, F.H. Gage, R. Riek, In vivo demonstration that alpha-synuclein oligomers are toxic, Proc. Natl. Acad. Sci. U. S. A. 108 (2011) 4194–4199.
[10] E. Rockenstein, S. Nuber, C.R. Overk, K. Ubhi, M. Mante, C. Patrick, A. Adame, M. Trejo-Morales, J. Gerez, P. Picotti, P.H. Jensen, S. Campioni, R. Riek, J. Winkler, F.H. Gage, B. Winner, E. Masliah, Accumulation of oligomer-prone alpha-synuclein exacerbates synaptic and neuronal degeneration in vivo, Brain 137 (2014) 1496–1513.
[11] O. Hwang, Role of oxidative stress in Parkinson's disease, Exp. Neurobiol. 22 (2013) 11–17.
[12] B.I. Giasson, J.E. Duda, I.V. Murray, Q. Chen, J.M. Souza, H.I. Hurtig, H. Ischiropoulos, J.Q. Trojanowski, V.M. Lee, Oxidative damage linked to neurodegeneration by selective alpha-synuclein nitration in synucleinopathy lesions, Science 290 (2000) 985–989.
[13] E. Sofic, K.W. Lange, K. Jellinger, P. Riederer, Reduced and oxidized glutathione in the substantia nigra of patients with Parkinson's disease, Neurosci. Lett. 142 (1992) 128–130.
[14] D.A. Bosco, D.M. Fowler, Q. Zhang, J. Nieva, E.T. Powers, P. Wentworth Jr., R.A. Lerner, J.W. Kelly, Elevated levels of oxidized cholesterol metabolites in Lewy body disease brains accelerate alpha-synuclein fibrilization, Nat. Chem. Biol. 2 (2006) 249–253.
[15] A. Yoritaka, N. Hattori, K. Uchida, M. Tanaka, E.R. Stadtman, Y. Mizuno, Immunohistochemical detection of 4-hydroxynonenal protein adducts in Parkinson disease, Proc. Natl. Acad. Sci. U. S. A. 93 (1996) 2696–2701.
[16] E. Dalfo, I. Ferrer, Early alpha-synuclein lipoxidation in neocortex in Lewy body diseases, Neurobiol. Aging 29 (2008) 408–417.
[17] R.J. Castellani, G. Perry, S.L. Siedlak, A. Nunomura, S. Shimohama, J. Zhang, T. Montine, L.M. Sayre, M.A. Smith, Hydroxynonenal adducts indicate a role for lipid peroxidation in neocortical and brainstem Lewy bodies in humans, Neurosci. Lett. 319 (2002) 25–28.
[18] D.I. Dryanovski, J.N. Guzman, Z. Xie, D.J. Galteri, L.A. Volpicelli-Daley, V.M. Lee, R.J. Miller, P.T. Schumacker, D.J. Surmeier, Calcium entry and alpha-synuclein inclusions elevate dendritic mitochondrial oxidant stress in dopaminergic neurons, J. Neurosci. 33 (2013) 10154–10164.
[19] J.R. Cannon, K.D. Geghman, V. Tapias, T. Sew, M.K. Dail, C. Li, J.T. Greenamyre, Expression of human E46K-mutated alpha-synuclein in BAC-transgenic rats replicates early-stage Parkinson's disease features and enhances vulnerability to mitochondrial impairment, Exp. Neurol. 240 (2013) 44–56.
[20] D. Lin, H.G. Lee, Q. Liu, G. Perry, M.A. Smith, L.M. Sayre, 4-Oxo-2-nonenal is both more neurotoxic and more protein reactive than 4-hydroxy-2-nonenal, Chem. Res. Toxicol. 18 (2005) 1219–1231.
[21] T. Näsström, T. Wahlberg, M. Karlsson, F. Nikolajeff, L. Lannfelt, M. Ingelsson, J. Bergström, The lipid peroxidation metabolite 4-oxo-2-nonenal cross-links alpha-synuclein causing rapid formation of stable oligomers, Biochem. Biophys. Res. Commun. 378 (2009) 872–876.
[22] T. Näsström, T. Fagerqvist, M. Barbu, M. Karlsson, F. Nikolajeff, A. Kasrayan, M. Ekberg, L. Lannfelt, M. Ingelsson, J. Bergström, The lipid peroxidation products 4-oxo-2-nonenal and 4-hydroxy-2-nonenal promote the formation of alpha-synuclein oligomers with distinct biochemical, morphological, and functional properties, Free Radic. Biol. Med. 50 (2011) 428–437.
[23] Z. Qin, D. Hu, S. Han, S.H. Reaney, D.A. Di Monte, A.L. Fink, Effect of 4-hydroxy-2-nonenal modification on alpha-synuclein aggregation, J. Biol. Chem. 282 (2007) 5862–5870.
[24] E.J. Bae, D.H. Ho, E. Park, J.W. Jung, K. Cho, J.H. Hong, H.J. Lee, K.P. Kim, S.J. Lee, Lipid peroxidation product 4-hydroxy-2-nonenal promotes seeding-capable oligomer formation and cell-to-cell transfer of alpha-synuclein, Antioxid. Redox Signal 18 (2013) 770–783.
[25] W. Xiang, J.C. Schlachetzki, S. Helling, J.C. Bussmann, M. Berlinghof, T.E. Schaffer, K. Marcus, J. Winkler, J. Klucken, C.M. Becker, Oxidative stress-induced posttranslational modifications of alpha-synuclein: specific modification of alpha-synuclein by 4-hydroxy-2-nonenal increases dopaminergic toxicity, Mol. Cell. Neurosci. 54 (2013) 71–83.
[26] H.A. Lashuel, C.R. Overk, A. Oueslati, E. Masliah, The many faces of alpha-synuclein: from structure and toxicity to therapeutic target, Nat. Rev. Neurosci. 14 (2013) 38–48.
[27] P.J. McLean, H. Kawamata, S. Ribich, B.T. Hyman, Membrane association and protein conformation of alpha-synuclein in intact neurons. Effect of Parkinson's disease-linked mutations, J. Biol. Chem. 275 (2000) 8812–8816.
[28] H. Esterbauer, R.J. Schaur, H. Zollner, Chemistry and biochemistry of 4-hydroxynonenal, malonaldehyde and related aldehydes, Free Radic. Biol. Med. 11 (1991) 81–128.
[29] D.E. Ehrnhoefer, J. Bieschke, A. Boeddrich, M. Herbst, L. Masino, R. Lurz, S. Engemann, A. Pastore, E.E. Wanker, EGCG redirects amyloidogenic polypeptides into unstructured, off-pathway oligomers, Nat. Struct. Mol. Biol. 15 (2008) 558–566.
[30] C.L. Pham, S.L. Leong, F.E. Ali, V.B. Kenche, A.F. Hill, S.L. Gras, K.J. Barnham, R. Cappai, Dopamine and the dopamine oxidation product 5,6-dihydroxylindole promote distinct on-pathway and off-pathway aggregation of alpha-synuclein in a pH-dependent manner, J. Mol. Biol. 387 (2009) 771–785.
[31] D.P. Hong, A.L. Fink, V.N. Uversky, Structural characteristics of alpha-synuclein oligomers stabilized by the flavonoid baicalein, J. Mol. Biol. 383 (2008) 214–223.
[32] T. Fagerqvist, T. Nasstrom, E. Ihse, V. Lindstrom, C. Sahlin, S.M. Tucker, A. Kasaryan, M. Karlsson, F. Nikolajeff, H. Schell, T.F. Outeiro, P.J. Kahle, L. Lannfelt, M. Ingelsson, J. Bergström, Off-pathway alpha-synuclein oligomers seem to alter alpha-synuclein turnover in a cell model but lack seeding capability in vivo, Amyloid 20 (2013) 233–244.